

Chapter 3: The Formation of the Solar Spectrum

3.1: The Solar Spectrum

The solar spectrum is our major observational tool for investigating conditions in the photosphere; the formation of the spectrum must be known if we wish to know how it is affected by these conditions. First we can examine the basic methods for dealing with the transfer of radiation through a medium, and then see how this applies to the formation of the solar spectrum, both for the continuum and for spectral lines.

3.2: Radiation Transfer

3.2.1: Basic Definitions

The radiation field is described by the **specific intensity** I_λ , the amount of energy per unit wavelength¹ interval in a beam radiating into a unit solid angle, passing through a unit area normal to the observer in unit time. Thus, the energy dE_λ in a wavelength interval $d\lambda$ passing through an area element $\cos\theta dA$, where θ is the angle between the normal to the area dA and the direction to the observer, is given by

$$dE_\lambda = I_\lambda \cos\theta dA d\lambda d\omega dt. \quad (3-1)$$

¹A similar, but slightly different formulation results if we use a unit frequency interval.

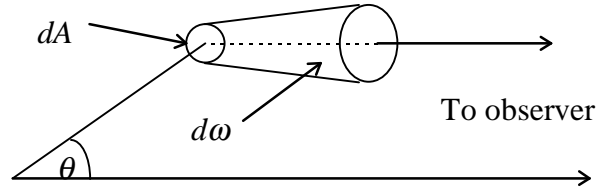


Figure 3-1: Geometry of variables in equation (3-1)

In general, the specific intensity will be a function of time, position and direction as well as wavelength.

As a beam of radiation travels a distance ds through a medium, photons will be removed from the beam by absorption and scattering. This can be characterised by a **mass absorption coefficient** or **opacity** κ_λ such that

$$dI_\lambda^- = -\rho\kappa_\lambda I_\lambda ds \quad (3-2)$$

where ρ is the density of the medium. In the photosphere, the opacity will be isotropic.

Photons will also be added to the beam by emission and scattering, with a **mass emission coefficient** or **emissivity** j_λ .

$$dI_\lambda^+ = \rho j_\lambda ds \quad (3-3)$$

Emission in the photosphere will be isotropic. The scattering contribution to the emissivity will in general depend on the specific intensity in all directions and at all wavelengths, but can usually be neglected.

These processes then give the basic equation governing the change in the radiation field caused by a medium,

$$dI_\lambda = (j_\lambda - \kappa_\lambda I_\lambda) \rho ds. \quad (3-4)$$

We now define the **source function** as the ratio of emissivity to opacity:

$$S_\lambda = \frac{j_\lambda}{\kappa_\lambda}. \quad (3-5)$$

The radiative transfer equation then becomes

$$dI_\lambda = (S_\lambda - I_\lambda) \rho \kappa_\lambda ds. \quad (3-6)$$

Then, if the properties of the medium are known, this equation can be solved with suitable boundary conditions to find the radiation field at any point.

3.2.2: The Plane Parallel Approximation

Since the photosphere is very thin (only a few hundred kilometres thick) compared to the radius of the sun (about 7×10^5 km), a small area of the photosphere can be treated as flat. As the properties of the photosphere vary strongly with height, it is natural to consider the photosphere to be composed of plane-parallel layers.

These layers are often considered to be homogeneous. As far as large scale velocity fields are concerned, this will rarely be an adequate approximation, even if the pressure, temperature and so on are sufficiently uniform, but a small (compared to the large scale motions) region can be treated as being composed of homogeneous plane-parallel layers. Thus, even if the photosphere is insufficiently homogeneous to be considered plane parallel, a small enough region will be sufficiently uniform, and the problem is then reduced to calculating the radiation emergent from all such different regions².

3.2.3: Radiation Transfer in a Plane Parallel Atmosphere

In a plane-parallel atmosphere, the path length ds (see figure 3-2) is related to the change in height by

$$ds = \frac{dz}{\mu} \quad (3-7)$$

where

$$\mu = \cos \theta \quad (3-8)$$

and θ is the angle between the direction of travel of the radiation and the normal to the surface.

²This is the basic principle behind multiple-stream models of the photosphere. Obviously, if we have a large number of streams or regions, the calculation of emergent spectra can be troublesome, so in general, such atmospheres are constructed so as to have as few regions as necessary. The actual use of such models is discussed in chapter 8.

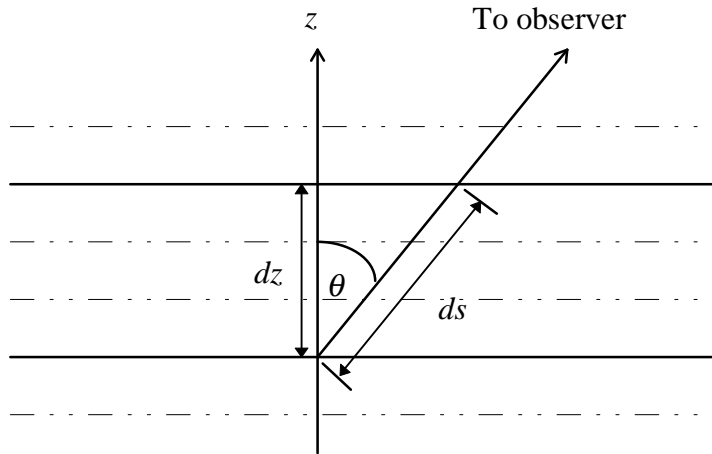


Fig 3-2: Geometry of a Plane Parallel Atmosphere

The monochromatic **optical depth** τ_λ is defined by

$$d\tau_\lambda = -\rho\kappa_\lambda dz \quad (3-9)$$

and, since $\tau_\lambda = 0$ at the observer ($z \approx \infty$),

$$\tau_\lambda(z) = \int_z^\infty \rho(z')\kappa_\lambda(z')dz'. \quad (3-10)$$

The transfer equation can then be written in its standard form for a plane-parallel atmosphere:

$$\mu \frac{dI_\lambda}{d\tau_\lambda} = I_\lambda - S_\lambda. \quad (3-11)$$

Then, with suitable boundary conditions, the intensity at any point can be calculated if the variation of the source function with S_λ optical depth is known. Thus, a model atmosphere can be created and adjusted until the calculated emergent intensity agrees with the observed intensity for all wavelengths and disk positions μ . If suitable wavelengths are used for comparison, we need only consider the continuous opacity and emission, and how these are affected by conditions in the photosphere, rather than taking into account the formation of spectral lines.

Once a model atmosphere is available, the formation of spectral lines can be considered in detail. Analysis of the formation of spectral lines can also be used to improve the model atmosphere, especially with regard to velocity fields present in the photosphere.

3.3: Spectral Line Formation

3.3.1: The Transfer Equation

At any wavelength, there will be two sources of opacity and emission: transitions between discrete energy levels which will give rise to spectral lines, and transitions between continuous energy levels or between a discrete energy level and continuous levels which will give rise to the continuum. We can consider these effects separately by noting their contribution to the total opacity and emissivity:

$$\kappa_{\lambda} = \kappa_{\lambda c} + \kappa_{\lambda \ell} \quad (3-12)$$

$$j_{\lambda} = j_{\lambda c} + j_{\lambda \ell} \quad (3-13)$$

where the subscripts c and ℓ denote the contributions from continuum and line transitions respectively. We can then define a continuum source function and a line source function in terms of the continuum and line opacities and emissivities:

$$S_{\lambda c} = \frac{j_{\lambda c}}{\kappa_{\lambda c}} \quad (3-14)$$

$$S_{\lambda \ell} = \frac{j_{\lambda \ell}}{\kappa_{\lambda \ell}} \quad (3-15)$$

The combined source function is then

$$S_{\lambda} = \frac{\kappa_{\lambda c} S_{\lambda c} + \kappa_{\lambda \ell} S_{\lambda \ell}}{\kappa_{\lambda c} + \kappa_{\lambda \ell}} \quad (3-16)$$

If the continuum and line source functions and opacities can be found at all optical depths, then the combined source function and the total opacity can be readily determined.

3.3.2: The Continuum Source Function and Scattering

The treatment of radiative transfer has so far largely ignored scattering; if scattering can be ignored, a simpler formulation results. The validity of neglecting scattering can be investigated by examining scattering processes in the photosphere.

Continuous scattering processes are **Thomson scattering** (scattering by free electrons) and **Rayleigh scattering** by atoms and molecules. Scattering processes are

distinct from absorption processes in that the photon is not destroyed, but both its energy and direction can be altered.

If we consider an electron oscillator driven by an electromagnetic field, the instantaneous power radiated by the accelerating electron is

$$P = \frac{2e^2 |\ddot{\mathbf{x}}|^2}{3c^3} \quad (3-17)$$

and, as this acceleration is provided by the driving field, it must be given by

$$\ddot{\mathbf{x}} = \frac{e}{m_e} \mathbf{E}_0 \cos \omega t. \quad (3-18)$$

The radiated power is then

$$P = \frac{2e^4}{3m_e^2 c^3} E_0^2 \cos^2 \omega t. \quad (3-19)$$

Averaging over an entire cycle, the average power emitted is

$$\bar{P} = \frac{e^4}{3m_e^2 c^3} E_0^2. \quad (3-20)$$

The specific intensity (in terms of the angular frequency) of the driving field is

$$I(\omega) = \frac{cE_0^2}{8\pi}. \quad (3-21)$$

The average power emitted by the electron must be the power scattered from the driving field; the scattered power must be related to the intensity by a scattering coefficient σ_T .

$$\bar{P} = \sigma_T I(\omega). \quad (3-22)$$

From equations (3-20), (3-21) and (3-22), it can be seen that the microscopic scattering coefficient for Thomson scattering, σ_T , is given by

$$\begin{aligned} \sigma_T &= \frac{8\pi e^4}{3m_e c^4} \\ &= 6.65 \times 10^{-25} \text{ cm}^2. \end{aligned} \quad (3-23)$$

This is independent of the wavelength of the incident field. This microscopic coefficient can be converted to a macroscopic mass scattering coefficient by multiplying it by the electron density per unit mass:

$$\kappa_e = \frac{N_e}{\rho} \sigma_T. \quad (3-24)$$

The importance of Thomson scattering in the photosphere can be seen when the electron mass scattering coefficient is compared to the total opacity (see table 3-1 below).

Table 3-1: Photospheric Scattering and Opacity

Optical Depth at 5000 Å τ_0	Electron Scattering Coefficient κ_e	Opacity at 5000 Å κ_0
0.001	3.38×10^{-13}	1.42×10^{-2}
0.01	1.13×10^{-12}	4.02×10^{-2}
0.1	4.31×10^{-12}	0.114
1.0	5.41×10^{-11}	0.804
10	1.05×10^{-9}	9.82

We can readily see that Thomson scattering is insignificant compared to the other processes responsible for the continuous opacity.

Due to the high abundance of neutral atomic hydrogen in the ground state in the photosphere, it will be the most important Rayleigh scatterer. We can consider the electron to be a driven oscillator, where

$$\ddot{\mathbf{x}} = \frac{e}{m_e} \mathbf{E}_0 \cos \omega t - \omega_0^2 \mathbf{x} \quad (3-25)$$

where ω_0 is the frequency of the transition responsible for the scattering. A solution to this differential equation is

$$\mathbf{x} = \frac{e}{m_e} \frac{\mathbf{E}_0 \cos \omega t}{(\omega^2 - \omega_0^2)} \quad (3-26)$$

which gives an average radiated power of

$$\bar{P} = \frac{e^4}{3m_e^2 c^3} \frac{\omega^4 E_0^2}{(\omega^2 - \omega_0^2)^2}. \quad (3-27)$$

This then gives a microscopic scattering coefficient of

$$\sigma_R = \sigma_T \frac{\omega^4}{(\omega^2 - \omega_0^2)^2}. \quad (3-28)$$

This must, however, be corrected for the strength of the transition by using an appropriate oscillator strength (such as is done with line opacity in section 3.3.5 below), giving

$$\sigma_{Rij} = \sigma_T f_{ij} \frac{\omega^4}{(\omega^2 - \omega_0^2)^2}. \quad (3-29)$$

If the incident frequency is much less than the transition frequency, the scattering is proportional to ω^4 , or λ^{-4} . Thus, we can expect Rayleigh scattering to be much more important for short wavelengths than for longer ones. As the hydrogen number density is much greater than the electron number density, we can expect Rayleigh scattering to be more important. The macroscopic scattering coefficient for hydrogen can be found by adding the contributions due to all of the transitions to the ground state.

The Rayleigh scattering will still be small compared to the continuous absorption in the photosphere. (See table 3-2.) For cooler stars, it can be important at short wavelengths. (Rayleigh scattering by H_2 can also be important in such cases.)

Table 3-2: Photospheric Scattering and Opacity

Optical Depth at 5000 Å τ_0	Rayleigh Scattering Coefficient for H $\kappa_{RH\ 5000\text{Å}}$	Opacity at 5000 Å κ_0
0.001	1.2×10^{-11}	1.42×10^{-2}
0.01	4.3×10^{-11}	4.02×10^{-2}
0.1	1.4×10^{-10}	0.114
1.0	3.2×10^{-10}	0.804
10	3.6×10^{-10}	9.82

The importance of scattering is also proportional to the non-isotropy of the radiation field. If the radiation field is isotropic, or nearly so, the energy scattered from the field propagating in a particular direction will be same as the energy scattered from other directions into this.

In LTE, neglecting scattering, the source function is given by the Planck function, so

$$S_{\lambda c} = B_{\lambda} = \frac{2hc^2}{\lambda^5} \frac{1}{e^{hc/\lambda kT} - 1}. \quad (3-30)$$

Since the processes responsible for continuous emission and absorption in the visible region of the spectrum are in LTE, this proves to be an adequate approximation, and is a most useful approximation, as it allows determination of the source function without reference to the radiation field. If scattering could not be neglected, the source function would depend on the specific intensity in all directions, which would greatly complicate the problem.

3.3.3: The Continuum Opacity

The continuous opacity of the photosphere is greatest at a wavelength of 8200 Å. The opacity in the visible and infrared spectrum is dominated by the H⁻ ion. The second electron in the H⁻ ion has two stable states with binding energies of 0.754 eV and 0.29 eV. The wavelengths corresponding to these ionisation energies are 1.645 μ and 4.3 μ. Although the H⁻ ion is not as abundant as neutral hydrogen, it has a large interaction cross-section, and is the dominant source of continuous emission and absorption in the visible spectrum due its dissociation and recombination. At wavelengths longer than 1 μ, free-free transitions are important to the opacity, with strongly increasing opacity towards the far infra-red.

Photo-ionisation of the more abundant absorbers, mainly neutral hydrogen, the H₂⁺ molecule, Mg and Si, is also important, especially at shorter wavelengths.

Since many more atomic species are liable to be photo-ionised by the higher energy photons in the far ultra-violet, it is not surprising that the ultra-violet continuous opacity is much higher than the visible and infra-red opacities.

3.3.4: The Line Source Function

The total emission at a wavelength is given by the Einstein spontaneous emission rate A_{21} :

$$j_{\lambda l} = \frac{hc^2}{4\pi\lambda^3} N_2 A_{21} \quad (3-31)$$

where N_2 is the population of the upper level of the transition per unit mass of the medium. The net absorption rate is given by the photo-excitation rate, B_{12} , from the lower level to the upper level, and the stimulated emission rate, B_{21} , from the upper level to the lower level:

$$\kappa_{\lambda\ell} = \frac{hc}{4\pi\lambda} (N_1 B_{12} - N_2 B_{21}) \quad (3-32)$$

where N_1 and N_2 are the lower and upper level populations respectively.

The line source function is then

$$S_{\lambda\ell} = \frac{N_2 A_{21}}{N_1 B_{12} - N_2 B_{21}} \quad (3-33)$$

which, using the Einstein relations

$$A_{21} = \frac{2hc^2}{\lambda^5} B_{21} \quad (3-34)$$

and

$$g_1 B_{12} = g_2 B_{21} \quad (3-35)$$

where g_1 and g_2 are the statistical weights of the lower and upper levels, can be rewritten as

$$S_{\lambda\ell} = \frac{2hc^2}{\lambda^5} \left(\frac{N_1 g_2}{N_2 g_1} - 1 \right)^{-1}. \quad (3-36)$$

If the level populations can be determined, the line source function will be known. In general, the level populations will need to be found by considering the transition rates from the upper and lower levels to each other and to and from all bound and continuum states. The problem can be simplified if only the strongest bound-bound transitions are considered. Often, especially if no strong transitions affect the levels, the populations are very close to their LTE values (the LTE approximation), so

$$\frac{N_2}{N_1} = \frac{g_2}{g_1} e^{-hc/\lambda kT}. \quad (3-37)$$

The line source function in LTE is then

$$S_{\lambda\ell} = \frac{2hc^2}{\lambda^5} \frac{1}{e^{hc/\lambda kT} - 1} = B_{\lambda} \quad (3-38)$$

and the combined LTE source function is

$$S_{\lambda} = \frac{\kappa_{\lambda c} B_{\lambda} + \kappa_{\lambda\ell} B_{\lambda}}{\kappa_{\lambda c} + \kappa_{\lambda\ell}} = B_{\lambda}. \quad (3-39)$$

3.3.5: The Line Opacity

Classically, the atom can be considered to act as a damped simple harmonic oscillator driven by an electromagnetic field. This gives a total atomic absorption cross-section of

$$\sigma_{total} = \frac{\pi e^2}{m_e c} \quad (3-40)$$

where e and m_e are the charge and mass of the electron. A more realistic quantum mechanical model of the atom can be used to find the total absorption cross-section for a transition between two levels i and j , which can then be written in a similar form,

$$\sigma_{total} = \frac{\pi e^2}{m_e c} f_{ij} \quad (3-41)$$

where f_{ij} is the oscillator strength or f-value of the transition. The f-value is related to the transition rate B_{ij} by

$$f_{ij} = \frac{hm_e c^3}{4\pi^2 e^2 \lambda^3} B_{ij} \quad (3-42)$$

and the f-values for the upwards and downwards transitions are related by

$$g_i f_{ij} = g_j f_{ji} \quad (3-43)$$

The opacity can thus be found in terms of the f-value of the upwards transition using equation (3-32) to give

$$\kappa_{\lambda\ell} = \frac{\pi e^2}{m_e c} f_{12} N_1 \left(1 - \frac{N_2 g_1}{N_1 g_2} \right) \quad (3-44)$$

where the factor $\left(1 - \frac{N_2 g_1}{N_1 g_2} \right)$ can be considered to be a correction for stimulated emission which, in LTE using equation (3-37), becomes $(1 - e^{-hc/\lambda kT})$.

The line opacity can then be found if the f-value for the transition and the population distribution of absorbers is known. The f-value can be calculated for a sufficiently simple atom (such as hydrogen), but only approximate values can be found for more complex atoms. Where accurate f-values are needed for complex atoms such as iron, it has so far proved more fruitful to determine them experimentally.

The difficulty in determining the line opacity lies in determining the population of absorbers capable of making a transition of a particular wavelength. If LTE can be reasonably assumed, this becomes much simpler.

3.3.6: The Line Profile Function for Stationary Non-Interacting Atoms

Although we might initially expect the total population of the level to be capable of making the transition at only one wavelength, there will be a spread of wavelengths for the transition, leading to a wavelength distribution of absorbers capable of making the transition. This distribution can be written in terms of a line profile function $\phi(\lambda)$:

$$N_\lambda = N_1 \phi(\lambda). \quad (3-45)$$

The previous results assumed that there was no spread of transition wavelengths, but will still be correct as the emission and absorption profiles are equal. In LTE the total level population will be given by a Boltzmann distribution, so

$$\kappa_{\lambda\ell} = \frac{\pi e^2}{m_e c} g_1 f_{12} \frac{e^{-hc/\lambda kT}}{U(T)} (1 - e^{-hc/\lambda kT}) \phi(\lambda) \quad (3-46)$$

All of the wavelength dependent information about the opacity is contained in the line profile function.

Even if we take an isolated atom, and carefully observe it, if we measure the energy of a state i , we will only measure a spread of energies due to the Heisenberg Uncertainty Principle. The energy spread will depend on the lifetime of the level in question.

The probability distribution of the level energy $W(E)$ can be obtained from the wavefunction for the occupation of the state, as

$$W(E) = \frac{1}{\hbar} W(\Delta\omega) \quad (3-47)$$

and

$$W(\Delta\omega) \propto \psi(\Delta\omega)^* \psi(\Delta\omega) \quad (3-48)$$

where $\Delta\omega$ is the angular frequency corresponding to the energy shift from the mean energy of the level. The wavefunction $\psi(\Delta\omega)$ is the Fourier transform of the wavefunction $\psi(t)$.

If the rate of removal of atoms from the state is Γ (for an isolated atom, Γ is the sum of the spontaneous emission rates to all lower levels, and $\Gamma = \frac{1}{t_N}$ where t_N is the natural lifetime of the level), the probability that the state is still occupied at a time t after a transition at time $t = 0$ is given by

$$W(t) = \begin{cases} 0 & \text{for } t < 0 \\ e^{-\Gamma t} & \text{for } t \geq 0 \end{cases} \quad (3-49)$$

from which we can determine the wavefunction

$$\psi(t) = \begin{cases} 0 & \text{for } t < 0 \\ \psi_0 e^{-\frac{\Gamma}{2}t} & \text{for } t \geq 0 \end{cases} \quad (3-50)$$

The Fourier transform of this is

$$\begin{aligned} \psi(\Delta\omega) &= \int_0^{\infty} \psi_0 e^{-\frac{\Gamma}{2}t} e^{-i\Delta\omega t} dt \\ &= \frac{\psi_0}{-i\Delta\omega - \frac{\Gamma}{2}} \end{aligned} \quad (3-51)$$

which gives

$$\psi(\Delta\omega)^* \psi(\Delta\omega) = \frac{\psi_0^2}{(\Delta\omega)^2 + \left(\frac{\Gamma}{2}\right)^2} \quad (3-52)$$

which can then be normalised to give the desired result:

$$W(\Delta\omega) = \frac{\frac{\Gamma}{2\pi}}{(\Delta\omega)^2 + \left(\frac{\Gamma}{2}\right)^2}. \quad (3-53)$$

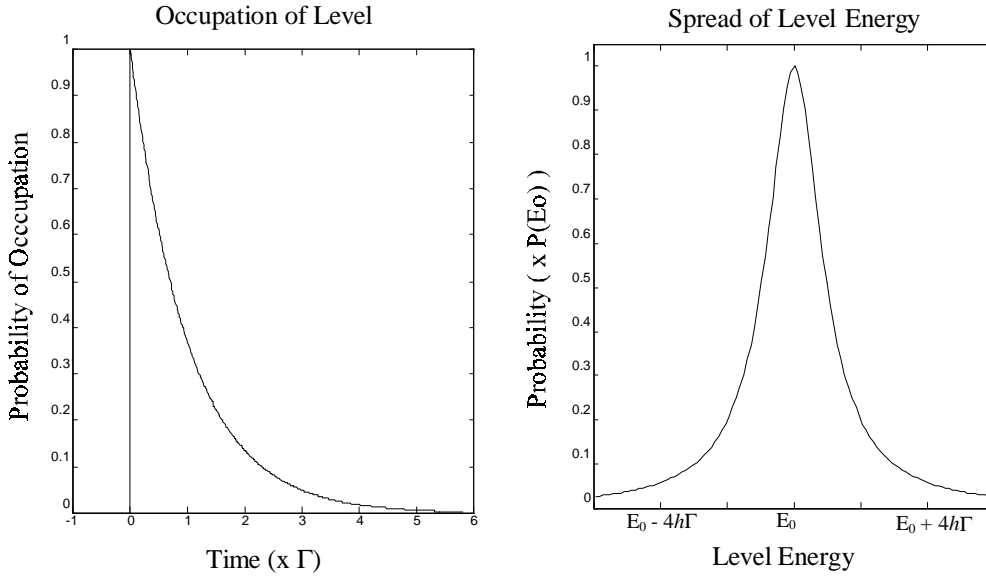


Fig 3-3: Effect of Finite Level Lifetime on Energy

The probability distribution for the energy (or frequency) of a transition between two such levels is given by a convolution of the energy probability distributions for each level, which gives us the line profile function in terms of $\Delta\omega$:

$$\begin{aligned}\phi(\Delta\omega) &= W_1(\Delta\omega) \otimes W_2(\Delta\omega) \\ &= \int_{-\infty}^{\infty} W_1(\omega') W_2(\Delta\omega - \omega') d\omega'.\end{aligned}\quad (3-54)$$

Substituting for W_1 and W_2 gives

$$\phi(\Delta\omega) = \frac{\Gamma_1 \Gamma_2}{4\pi^2} \int_{-\infty}^{\infty} \frac{d\omega'}{\left(\omega'^2 + \left(\frac{\Gamma_1}{2}\right)^2\right) \left((\Delta\omega - \omega')^2 + \left(\frac{\Gamma_2}{2}\right)^2\right)} \quad (3-55)$$

which can be calculated using the residue theorem, giving

$$\phi(\Delta\omega) = \frac{\frac{\Gamma_1 + \Gamma_2}{2}}{(\Delta\omega)^2 + \left(\frac{\Gamma_1 + \Gamma_2}{2}\right)^2} \quad (3-56)$$

We can now define a width for the transition as the sum of the widths of the upper and lower levels,

$$\Gamma = \Gamma_1 + \Gamma_2 \quad (3-57)$$

and rewrite $\Delta\omega$, the frequency difference from the transition frequency, as

$$\Delta\omega = 2\pi(\nu - \nu_0) \quad (3-58)$$

where ν_0 is the mean frequency of the transition, giving the Lorentz profile for the line in terms of frequency

$$\phi(\nu) = \frac{\frac{\Gamma}{4\pi^2}}{(\nu - \nu_0)^2 + \left(\frac{\Gamma}{4\pi}\right)^2} \quad (3-59)$$

or, if the width is small compared to the frequency (that is, $(\nu - \nu_0)$ is small compared to ν), we can convert to wavelength units and normalise, obtaining

$$\phi(\lambda) = \frac{\frac{\Delta\lambda}{2\pi}}{(\lambda - \lambda_0)^2 + \left(\frac{\Delta\lambda}{2}\right)^2} = \frac{c}{\lambda_0^2} \phi(\nu) \quad (3-60)$$

where $\Delta\lambda$ is the width of the profile in frequency units; $\Delta\lambda$ in terms of Γ is given by

$$\Delta\lambda = \frac{\lambda_0^2 \Gamma}{2\pi c}. \quad (3-61)$$

3.4: Spectral Line Profiles

The profiles of emergent spectral lines can now be calculated given:

- 1) sufficient information on physical conditions in the photosphere,
- 2) the oscillator strength or f-value for the transition and other atomic data needed to determine populations such as the excitation energy of the lower level, and
- 3) the line profile function.

The line profile function for stationary non-interacting atoms that we have found here, dependent only on the level lifetime, is only the starting point for finding the complete line profile function. The profile will be affected by motions which will cause changes in the transition wavelength due to the Doppler effect, and interactions between an absorber and other atoms, particles or fields can affect either the wavelength of the transition or the width. Interatomic interactions will be considered in detail in chapter 4, and the effects of velocities on the line profile function will be considered in the following sections.

At this point, it should be noted that although the line profile function does affect the emergent profile strongly, it is not the same as the emergent profile. The

emergent profile will be a combination of line profile functions from different depths and different areas of the photosphere, with the contribution being weighted by the local source function and the absorption due to the opacity of the overlying photospheric layers. Velocity gradients, both vertical and horizontal, will result in the various contributing line profile functions being shifted in wavelength with respect to each other.

3.5: Thermal Motions

Any material, even if stationary, will exhibit thermal motions of its constituent particles. For a gas in thermal equilibrium (or in LTE), the probability distribution of the particle speeds is the Maxwell speed distribution:

$$W(v) = 4\pi v^2 \left(\frac{m}{2\pi kT} \right)^{\frac{3}{2}} e^{-\frac{mv^2}{2kT}} \quad (3-62)$$

where m is the mass of the particle. The probability distribution for the line of sight velocity ξ is

$$W(\xi) = \frac{1}{\xi_0 \sqrt{\pi}} e^{-\left(\frac{\xi}{\xi_0}\right)^2} \quad (3-63)$$

where the most probable line of sight speed ξ_0 is given by

$$\xi_0 = \sqrt{\frac{2kT}{m}}. \quad (3-64)$$

The probability distribution for thermal Doppler shifts is then

$$W(\Delta\lambda)d\Delta\lambda = \frac{1}{\Delta\lambda_D \sqrt{\pi}} e^{-\left(\frac{\Delta\lambda}{\Delta\lambda_D}\right)^2} d\Delta\lambda \quad (3-65)$$

where

$$\Delta\lambda_D = \lambda_0 \frac{\xi_0}{c}. \quad (3-66)$$

If the stationary line profile function $\phi(\lambda)$ (see equation (3-60)) is uncorrelated with the velocity of the absorber, the line profile function taking thermal motion into account is given by the convolution of the original line profile and the Doppler shift distribution:

$$\begin{aligned}
\phi_D(\lambda) &= \phi(\lambda) \otimes W(\Delta\lambda) \\
&= \int_{-\infty}^{\infty} \phi(\lambda - \Delta\lambda) W(\Delta\lambda) d\Delta\lambda \\
&= \int_{-\infty}^{\infty} \frac{\frac{\Delta\lambda_L}{2\pi}}{(\lambda - \Delta\lambda - \lambda_0)^2 + \left(\frac{\Delta\lambda_L}{2}\right)^2} \frac{1}{\Delta\lambda_D \sqrt{\pi}} e^{-\left(\frac{\Delta\lambda}{\Delta\lambda_D}\right)^2} d\Delta\lambda \quad (3-67) \\
&= \pi^{-\frac{3}{2}} \frac{\Delta\lambda_L}{2\Delta\lambda_D} \int_{-\infty}^{\infty} \frac{e^{-\left(\frac{\Delta\lambda}{\Delta\lambda_D}\right)^2}}{\left(\frac{\lambda - \lambda_0}{\Delta\lambda_D} - \frac{\Delta\lambda}{\Delta\lambda_D}\right)^2 + \left(\frac{\Delta\lambda_L}{2\Delta\lambda_D}\right)^2} \frac{d\Delta\lambda}{\Delta\lambda_D}
\end{aligned}$$

into which we can make the natural substitutions

$$x = \frac{\Delta\lambda}{\Delta\lambda_D}, \quad (3-68)$$

$$a = \frac{\Delta\lambda_L}{2\Delta\lambda_D} \quad (3-69)$$

and

$$v = \frac{\lambda - \lambda_0}{\Delta\lambda_D}. \quad (3-70)$$

Thus, the line profile function becomes

$$\begin{aligned}
\phi_D(\lambda) &= U(a, v) \\
&= \frac{a}{\pi^{\frac{3}{2}}} \int_{-\infty}^{\infty} \frac{e^{-x^2}}{(v-x)^2 + a^2} dx \quad (3-71) \\
&= \frac{1}{\sqrt{\pi}} H(a, v)
\end{aligned}$$

where $H(a, v)$ and $U(a, v)$ are known as the **Voigt function** and the **normalised Voigt function** respectively.

Here, v is the number of Doppler widths that the wavelength is away from the line centre, and a is the ratio of the Lorentzian profile half-width to the Doppler full-width.

There are simple approximate methods by which the Voigt function can be calculated for large v and a , thus avoiding the need to directly numerically integrate.³

³See section 5.3.2 for details on the calculation of Voigt profiles.

3.6: Mass Motions

The solar mass motion of most importance is the granular flow. Not only is there a large scale granular flow (the actual granulation pattern), there are also smaller scale unresolved motions within each granule.

3.6.1: Small Scale Mass Motions

The necessary existence of small scale mass motions is a result of the extremely turbulent flow in the granulation. Its effects are also readily observed experimentally, as the Doppler width of spectral lines is larger than that expected from the thermal motions alone. These small scale motions are usually called **microturbulence**. Other than their existence and approximate speeds, it is difficult to extract information regarding these velocities from the solar spectrum, as difficulties result if the microturbulent velocity field varies with height or horizontal position in the photosphere. High spatial resolution spectra show that the microturbulence field does vary with horizontal position, with maximum microturbulence where the upwards flowing granular centre and the downwards flowing intergranular space meet.⁴ This is exactly the result expected for a highly turbulent convective cell that has not reached an equilibrium state with uniform microturbulence. The height dependence is not as easy to measure.

The actual line of sight velocity distribution is generally assumed to be Gaussian; this is the usual assumption made for highly turbulent flows.⁵ There is also

⁴Nesis, A., Hanslmeier, A., Hammer, R., Komm, R., Mattig, W. and Staiger, J. "Dynamics of Solar Granulation II: A Quantitative Approach" *Astronomy and Astrophysics* **279**, pg 599-609 (1993)

⁵There are indications that at any given characteristic length scale, the velocities cannot have a symmetric Gaussian distribution, as this would prevent the expected energy transfer from large to small scales from occurring, but as the asymmetric variation from a true Gaussian distribution should alternate as successively smaller characteristic length scales are reached, the asymmetry should become vanishingly small if a sufficient number of characteristic scales are considered simultaneously. Thus the velocity field should be very close to having a Gaussian distribution.

observational evidence to support this, as spectra calculated with this assumption are very similar to observed spectra. The line of sight velocity distribution will thus be given by

$$W(\xi) = \frac{1}{\xi_{\text{turb}} \sqrt{\pi}} e^{-\left(\frac{\xi}{\xi_{\text{turb}}}\right)^2}. \quad (3-72)$$

where ξ_{turb} is the most probable turbulent line of sight velocity (also called the **microturbulence** or the **microturbulent velocity**). This motion combined with the thermal motion gives a combined distribution

$$W(\xi) = \frac{1}{\left(\xi_{\text{thermal}}^2 + \xi_{\text{turb}}^2\right)^{\frac{1}{2}} \sqrt{\pi}} e^{-\left(\frac{\xi^2}{\xi_{\text{thermal}}^2 + \xi_{\text{turb}}^2}\right)}. \quad (3-73)$$

The small scale velocity field is therefore very easy to deal with, as it suffices to simply use the most probable combined speed

$$\xi_0 = \sqrt{\xi_{\text{thermal}}^2 + \xi_{\text{turb}}^2} \quad (3-74)$$

in place of the most probable thermal speed (which was used before considering turbulent motion).

Thus, the line profile taking the microturbulent velocity field into account is still given by a Voigt profile, but with the Doppler width of the profile increased accordingly. The most probable speed being a function of horizontal position and depth will result in the line profile function being dependent on the horizontal position as well as the height within the photosphere.

3.6.2: The Granular Flow

The large scale flow will also result in Doppler shifts. If we consider a volume of gas in this large scale flow, it will have some line of sight velocity V_G which will depend on the position within the granular cell. The particles making up this volume of gas will also have thermal and microturbulent motions, but the large scale velocity V_G will be the same for all of the particles. The resulting line profile function will be given by a convolution of all four items contributing to the line shape so far: the Lorentzian profile due to the natural line width, the thermal velocity distribution, the microturbulent velocity distribution, and the granular flow Doppler shift. The first three of these give a Voigt profile, and the fourth will merely shift the entire profile, preserving its shape exactly, giving

$$\begin{aligned}\varphi_G(\lambda) &= U(a, v) \\ &= \frac{1}{\sqrt{\pi}} H(a, v)\end{aligned}\quad (3-75)$$

with

$$\begin{aligned}v &= \frac{\lambda - \left(\lambda_0 - \lambda_0 \frac{V_G}{c} \right)}{\Delta\lambda_D} \\ &= \frac{\lambda - \lambda_0 (1 - V_G/c)}{\Delta\lambda_D}\end{aligned}\quad (3-76)$$

where V_G is the upwards velocity.

Unlike the microturbulent field, which could possibly be position independent⁶, the large scale flow field cannot be independent of horizontal position.⁷⁸ The

⁶Even though it turns out that the microturbulence is not uniform, and the non-uniformities are important, this variation is a consequence of the details of the fluid flow in the photosphere, not a result of basic geometry.

⁷As some of the material is moving upwards, and some is moving downwards, the vertical flow velocity must vary with position. Despite this, it is occasionally assumed (for example, Stathopoulou, M. and Alissandrakis, C.E. "A Study of the Asymmetry of Fe I Lines in the Solar Spectrum" *Astronomy and Astrophysics* **274**, pg 555-562 (1993)) that the large scale flow field is horizontally uniform, so as to be able to maintain a strictly plane-parallel photosphere.

⁸Note that this does not necessary overly complicate the calculation of spectra. See section 8.1 for the cases which remain simple. The horizontal variation of microturbulence is a greater complication.

complications that this introduces are dealt with in chapter 8. The large scale flow field must also be asymmetric⁹, a feature of prime importance for any study of asymmetry in solar spectral lines.

⁹A two-dimensional flow can be symmetric, but three-dimensional flows are generally asymmetric. As the areas of the photosphere occupied by upflows and downflows are not the same, the upwards and downwards flow velocities must be different.

